Biophysical Journal, Volume *120*

Supplemental information

Stability and conformation of the dimeric HIV-1 genomic RNA 5′UTR

Robert J. Blakemore, Cleo Burnett, Canessa Swanson, Siarhei Kharytonchyk, Alice Telesnitsky, and James B. Munro

Stability and conformation of the dimeric HIV-1 genomic RNA 5'UTR

Robert J. Blakemore[1,2], Cleo Burnett[3], Canessa Swanson[4], Siarhei Kharytonchyk[3], Alice Telesnitsky[3], and James B. Munro[1,5,6*]

[1]Department of Molecular Biology and Microbiology, Tufts University School of Medicine and School of Graduate Biomedical Sciences, Boston, MA, 02111, USA

[2]Graduate Program in Molecular Microbiology, Tufts University Graduate School of Biomedical Sciences, Boston, MA, 02111, USA

[3]Department of Microbiology and Immunology, University of Michigan Medical School, Ann Arbor, MI, 48109, USA

[4]Department of Chemistry and Biochemistry, University of Maryland Baltimore Country, Baltimore, MD, 21250, USA

[5]Department of Microbiology and Physiological Systems, University of Massachusetts Medical School, Worcester, MA, 01605, USA

[6]Department of Biochemistry and Molecules Pharmacology, University of Massachusetts Medical School, Worcester, MA, 01605, USA

*To whom correspondence should be addressed. Tel: +1 (774) 455-4754; Fax: +1 (508) 856-5920; Email: james.munro@umassmed.edu

Supporting Material

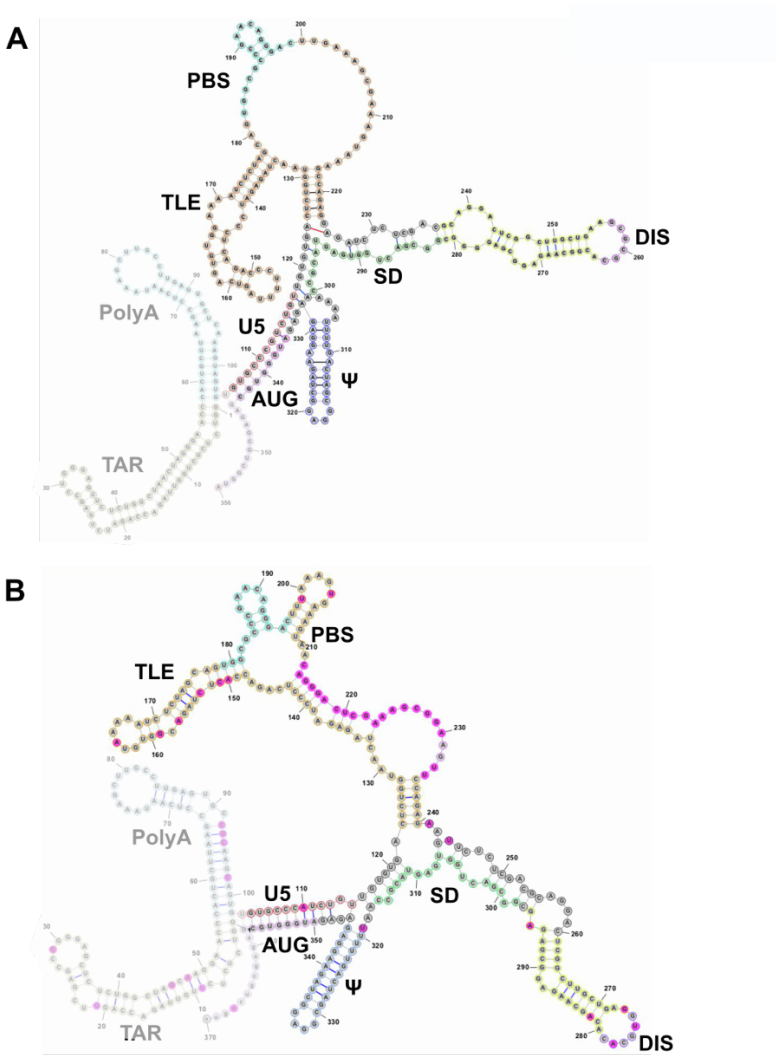

Fig. S1. Secondary structural models of the NL4.3-5'UTR and MAL-5'UTR. (**A**) Secondary structural model of the NL4.3-5'UTR with functional elements indicated: TAR, trans-acting response element; PolyA, polyadenylation signal; U5, unique 5' sequence; TLE, tRNA-like element; PBS, primer-binding site; DIS, dimerization initiation sequence; SD, splice donor; Ψ site; AUG, translation start site. The shaded sequence, containing TAR, PolyA, and a segment of the AUG hairpin, are not present in the NL4.3-5'UTR^{238} RNA construct studied here. (**B**) Secondary structural model of the MAL-5'UTR with functional elements indicated as in (A). Nucleotides highlighted in pink are distinct from NL4.3-5'UTR.

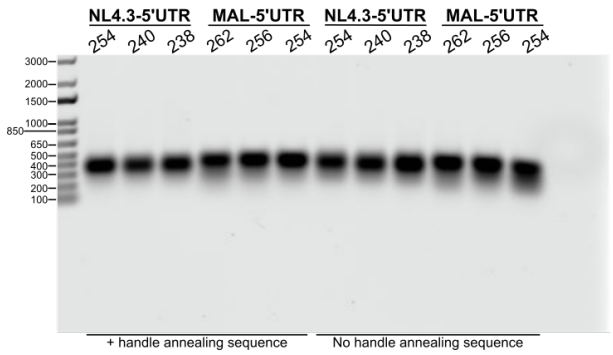

Fig. S2. Evaluation of RNA with denaturing gel electrophoresis. Purified *in-vitro* transcribed RNA was run on a denaturing 1% agarose gel in TAE with 1% bleach to evaluate purity. NL4.3-5'UTR^{238} and MAL-5'UTR^{254}, with and without the handle annealing sequence, were used in the present study.

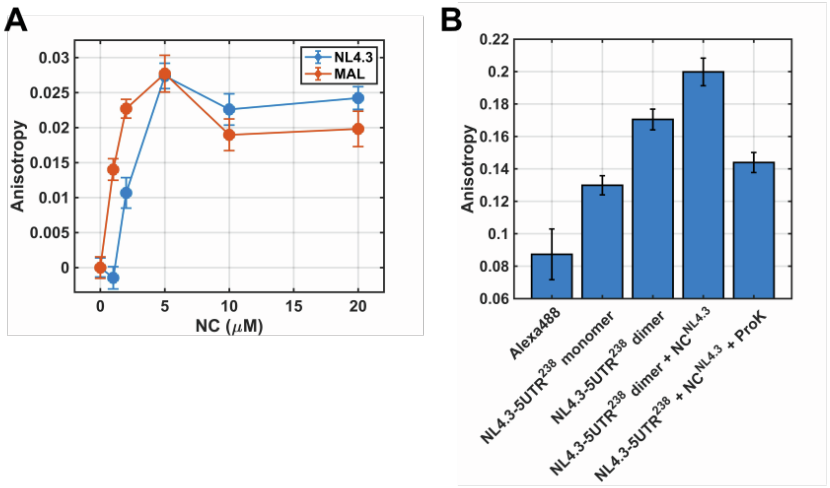

Fig. S3. Verification of NC binding to 5'UTR RNA with fluorescence anisotropy. (**A**) Steady-state fluorescence anisotropy acquired with NL4.3-5'UTR^{238} (blue) and MAL-5'UTR^{254} (orange) labeled with Alexa488 at the 3' terminus. 5'UTR RNA was dimerized in PI buffer at 1 mM Mg^{2+} for 1 hr at 37°C in the presence of varying concentrations of cognate NC protein (NC$^{NL4.3}$ or NC^{MAL}). Data are presented as the average change in anisotropy over three measurements with error bars reflecting the standard error. (**B**) Anisotropy of Alexa488-labeled NL4.3-5'UTR^{238} dimerized in the absence and presence of NC$^{NL4.3}$, and after removal of NC$^{NL4.3}$ with proteinase K (ProK). Data are presented as the average of three measurements with error bars reflecting the standard error.

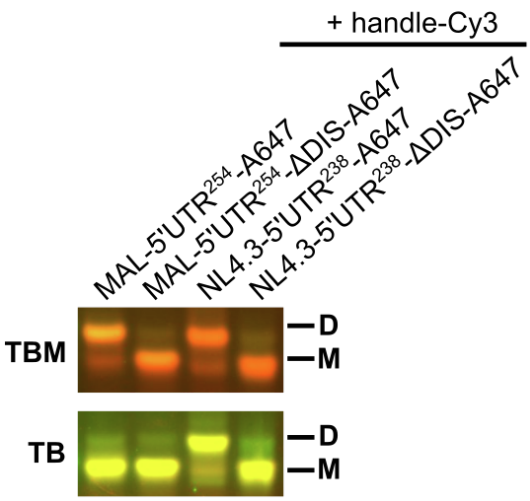

Fig. S4. Dimerization of fluorescently labeled 5'UTRs. Analysis of 5'UTR dimer stability with non-denaturing RNA gel electrophoresis. The indicated Alexa647-labeled RNA constructs were dimerized in the presence of the Cy3-labeled DNA oligonucleotide handle in PI buffer for 1 hr at 37°C, followed by evaluation on 1% agarose gels in TB or TBM buffers. Gels were imaged on a fluorescent gel scanner. Monomer (M) and dimer (D) species are indicated. In the NL4.3-5'UTR^{238} construct, the ΔDIS mutant contains a GAGA tetraloop in place of the DIS loop (44).

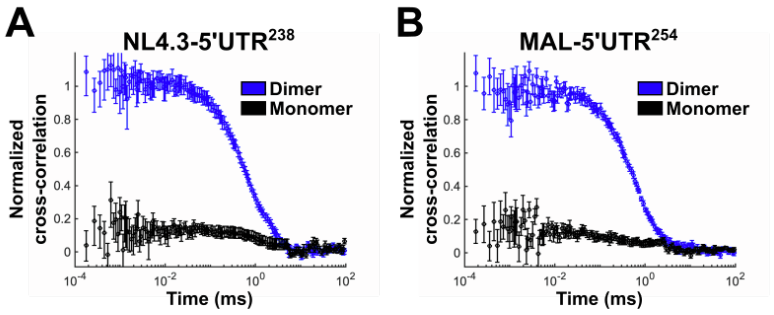

Fig. S5. Monomeric 5'UTR does not contribute to the FCCS measurement. (**A**) CC data for dimerized (blue) and monomeric (black) NL4.3-5'UTR^{238}. A 1:1 molar ratio of NL4.3-5'UTR^{238} labeled with either Alexa488 or Alexa647 was evaluated by FCCS before (monomeric) or after (dimeric) 1 hr incubation in PI buffer at 37°C. Only dimerized RNA leads to non-zero CC, consistent with diffusing complexes containing both fluorophores. (**B**) The same data for MAL-5'UTR^{254}. Here again, only dimerized RNA leads to non-zero CC. In both panels the data are presented as the average normalized CC from 10 measurements of 10 s duration each. Error bars reflect the standard error.

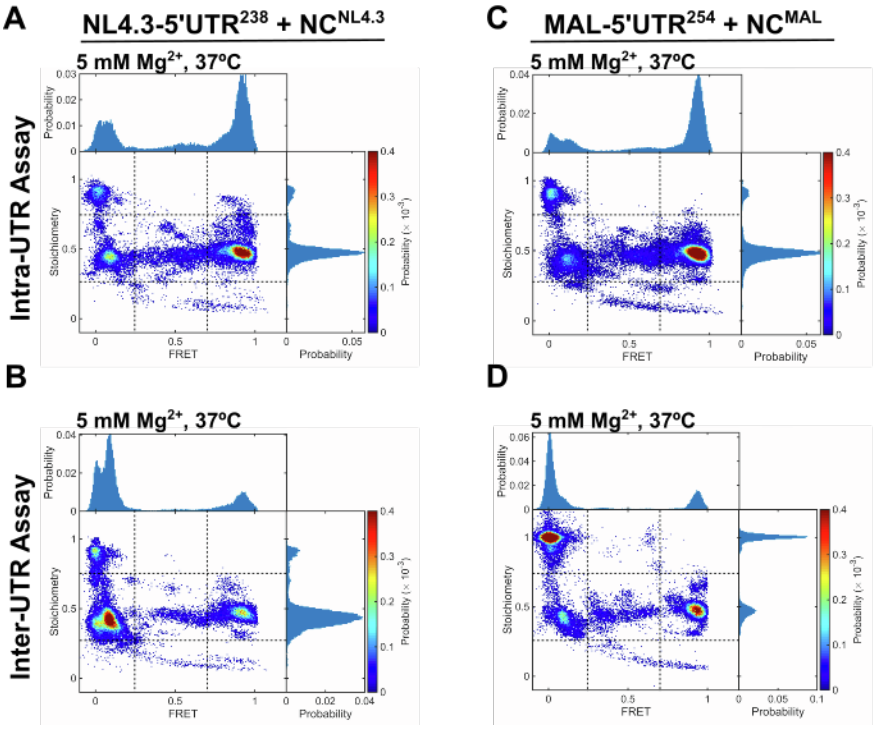

Fig. S6. smFRET analysis of the 5'UTR dimers formed at elevated Mg^{2+} concentration. All samples were dimerized in PI buffer at 5 mM Mg^{2+} in the presence of cognate NC for 1 hr at 37°C. Samples were imaged in the same buffer at room temperature. Bivariate ES plots and univariate histograms displaying the distributions of FRET efficiency and stoichiometry are presented as in **Figs. 6** and **8**. Data are shown for the NL4.3-5'UTR^{238} dimer acquired with the (**A**) Intra-UTR FRET Assay and the (**B**) Inter-UTR FRET Assay. Also shown are (**C**) Intra-UTR FRET data and (**D**) Inter-UTR FRET data for MAL-5'UTR^{254} dimers.

		Intra-UTR Assay			Inter-UTR Assay	
		NL4.3-5'UTR^{238}	MAL-5'UTR^{254}		NL4.3-5'UTR^{238}	MAL-5'UTR^{254}
1 mM Mg^{2+}, 37°C	DCM/KD	61%	48%	KD	58%	4%
	ED	18%	24%	ED	29%	15%
	Donor only	15%	17%	Donor only	11%	79%
	NA	6%	11%	NA	2%	2%
5 mM Mg^{2+}, 37°C	DCM/KD	69%	64%	KD	65%	11%
	ED	18%	21%	ED	20%	16%
	Donor only	9%	9%	Donor only	14%	71%
	NA	4%	7%	NA	<1%	2%
1 mM Mg^{2+}, 57°C	DCM/KD	13%	59%	KD	30%	9%
	ED	69%	26%	ED	51%	16%
	Donor only	15%	8%	Donor only	13%	72%
	NA	3%	7%	NA	6%	3%
1 mM Mg^{2+}, 37°C, $NC^{NL4.3}$	DCM/KD	17%	21%	KD	21%	20%
	ED	73%	71%	ED	60%	69%
	Donor only	9%	5%	Donor only	12%	4%
	NA	1%	2%	NA	7%	7%
5 mM Mg^{2+}, 37°C, $NC^{NL4.3}$	DCM/KD	60%	68%	KD	63%	14%
	ED	22%	17%	ED	24%	22%
	Donor only	10%	10%	Donor only	11%	61%
	NA	8%	6%	NA	3%	3%
1 mM Mg^{2+}, 37°C, 10 μM Neo	DCM/KD		66%	KD		79%
	ED		17%	ED		13%
	Donor only		10%	Donor only		5%
	NA		6%	NA		4%

Table S1. Summary of 5'UTR conformation occupancies determined through the Intra- and Inter-UTR smFRET Assays.